JOURNAL OF APPLIED ELECTROCHEMISTRY 26 (1996) 481–486

# Current distribution in aluminium electrolysis cells with Søderberg anodes
# Part I: Experimental study and estimate of anode consumption

Z. KUANG, J. THONSTAD

*Department of Electrochemistry, The Norwegian Institute of Technology, N-7034, Trondheim, Norway*

Received 14 August 1995; revised 29 September 1995

A voltage probe was used to determine the current distribution along the sides of the anodes in commercial Søderberg aluminium cells. The current density decreased in the upward direction along the side of the anode from 0.8 A $cm^{-2}$ on the working face to 0.15–0.28 A $cm^{-2}$ near the surface of the bath. It was estimated that only 5%–10% of the carbon dust formed in Søderberg cells was generated at the side of the anode, and the rest came from the working face of the anode. About 5% of the total anode consumption took place on the side of the anode, of which ~3% was caused by air-burning above the bath (electrolyte) level.

## 1. Introduction

There are two fundamental anode designs used in aluminium electrolysis: prebaked anodes and Søderberg anodes. Both anodes are formulated from the same raw materials (petroleum coke and coal tar pitch) and undergo the same primary cell reaction (Equation 1),

$$Al_2O_3 + 3/2C = 2Al + 3/2CO_2 \quad (1)$$

Prebaked anodes are formed and baked above 1100° C prior to use in the cell. In Søderberg cells, the anode paste (pitch–carbon mixture) is contained in a steel casing and it is baked in situ (self-baking) by the heat of the cell (~ 950° C). Electrical contact to the anode is provided by steel pins which are introduced through the anode paste. The paste is slowly converted to a carbonized mass when moving downward to hotter zones as a consequence of the anode consumption.

Compared to prebaked cells, Søderberg cells require lower capital investment and the cells have less operating disturbances due to the continuous anode. These advantages are outweighed by the inferior carbon quality (due to the lower baking temperature), which leads to a high anode carbon consumption and harmful emissions. The excess consumption, with respect to Faraday's law, is mainly composed of two parts: that is, excess carbon gasification (due to the Boudouard reaction, $C + CO_2 = 2CO$) and carbon dusting (detached carbon particles) [1, 2]. The carbon dust particles accumulate at the surface of the bath (electrolyte) or mix together with the bath, and the dust has a negative effect on the bath properties. The Boudouard reaction does not occur on the surface of the anode [3], but it may occur if the gas permeates the porous anode structure.

In our laboratory, extensive studies were carried out to investigate the dusting problem in Søderberg cells [2, 4]. These studies showed that the anode carbon consumption (and dusting) increases with decreasing anode current density [1, 2]. In an industrial cell, the current density is uniform on the working face of the anode, while it is lower on the side of the anode.

To determine the current distribution, the potential distribution in the bath was measured. Only a few works have been published on measurements of the potential distribution in industrial aluminium cells by using electrode probes. Haupin [5] demonstrated the use of a so-called scanning reference electrode. Thonstad and Rolseth [6] applied an electrode in studying the anodic oxidation of aluminium dissolved in cryolite melts by measuring current-voltage curves in industrial cells. Rolseth *et al.* [7] investigated the metal wave behaviour by placing a probe close to the metal-bath interface in a commercial cell.

In the present work, an electrode probe connected to a position sensor was used to measure the potential distribution in industrial Søderberg cells. By mapping the potential distribution in the bath, isopotential lines could be drawn, and the current distribution was derived from the isopotential lines. Based on the results of the current distribution and the results of the effect of current density on carbon consumption [1], dusting from the sides of the Søderberg anode of industrial cells could be estimated. For prebaked anodes, Cutshall [8] claimed that sloughing (i.e., dusting) occurs mainly on the sides of the anodes where the current density is low. The present investigation examines if this conclusion is valid for Søderberg cells.

0021-891X  

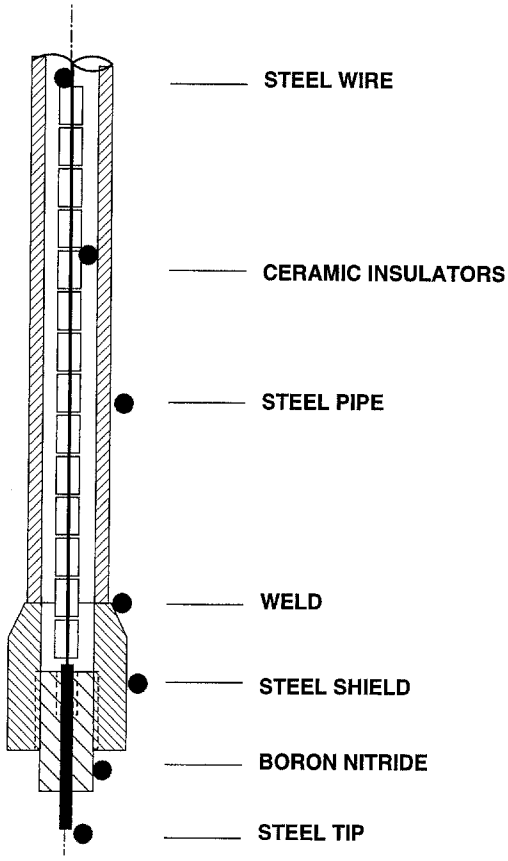


Fig. 1. Reference electrode probe.

By measuring the wear along the sides of industrial Søderberg anodes, the carbon consumption from the sides of the anode was estimated.

## 2. Experimental details

### 2.1. *Electrode probe*

To measure the potential distribution in the bath, a reference electrode probe was made as shown in Fig. 1. It was housed in a steel pipe with a head of thicker steel pipe to retard attack by aluminium. A boron nitride insulator was threaded into the head, so the 8 mm steel tip serving as probe projected through the boron nitride. The steel pipe was bent about 30 degrees, at a distance of 30 cm above the tip, to make it easier to reach various positions in the bath. Even so, it was difficult to measure under the curved part of the anode, so in this region the data were extrapolated.

Another steel rod was inserted into the liquid aluminium to serve as the counter electrode, so the potential at the tip of the electrode probe could be obtained, referred to the potential of the aluminium pool.

To make the probe work as an aluminium electrode, a thin coating of molten aluminium was applied to the tip of the probe by dipping it into the pool of molten metal in the cell for about 1–2 min prior to use. It has been shown in earlier works [4, 10] that this type of device works as an aluminium electrode, provided that the aluminium coating is renewed periodically. Our tests showed that the probe could keep a stable potential in the bath for about 8 min after dipping.

The probe lasted about half-an-hour in the bath before the potential readings became erratic. The probe might last longer if used with care, especially by avoiding attack by the molten aluminium on the shield of the probe. Some of the measured data were obviously incorrect, but it was difficult to establish the reason for these errors: either instability of the probe, the effect of gas bubbles, or the effect of waves on the molten metal. Such errors became more pronounced when the probe was moved close to the anode.

### 2.2. *Position sensor*

An accurate position sensor has been designed by Tørklep (Elkem Research, Kristiansand, Norway) [9] and the principle is shown schematically in Fig. 2. Two arms are linked by a universal joint (3) and connected to two other similar joints (2, 4). One of the end joints is connected to a rotatable joint which holds the probe. This design allows the probe to be moved freely. All the joints give electronic signals to a computer so that the angles are known. The movement of the probe tip is followed by recording the angular displacement of all seven physical axes (two per universal joint and one for the rotatable joint). As the equipment is calibrated by a reference system, the position of the probe tip can be known wherever it is placed. It could determine accurately the position of the tip of the sensing rod placed in the cell and store the data on floppy disks in spreadsheet-readable format. A more detailed description of this position sensor has been given by Tørklep [9].

The position sensor, or 'ledge scanner', was originally developed to measure ledge profiles (the profiles of the frozen bath which covers the walls of the cell). It was found that the position sensor could be

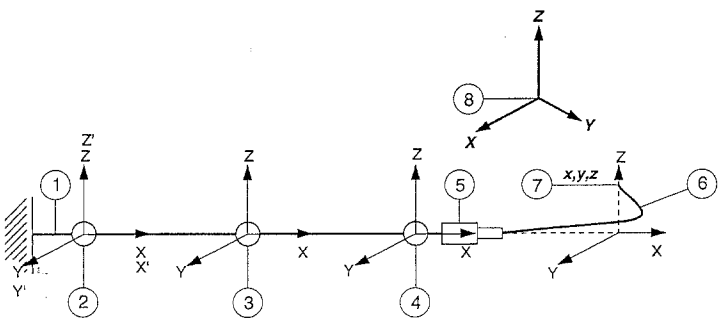


Fig. 2. Schematic view of the position sensor [9]. Key: (1) bracket supporter, (2, 3, 4) universal joints, (5) probe rod holder, rotatable joint, through 360°, (6) probe, (7) probe tip, (8) reference system.

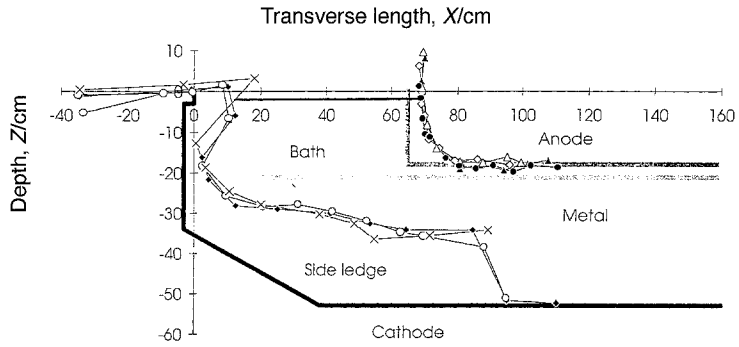


Fig. 3. Outline of a section of a measured Søderberg cell.

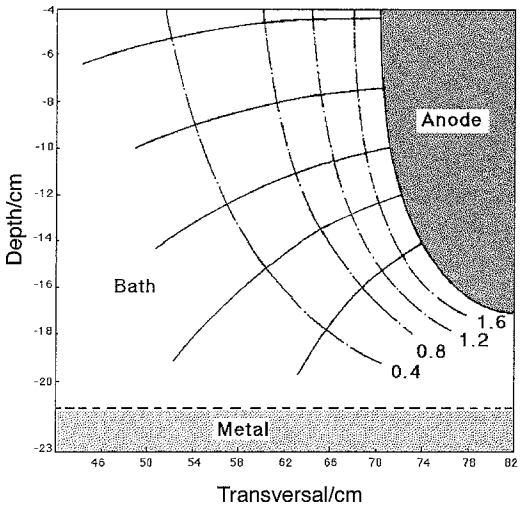


Fig. 4. A plot of equipotential lines and current lines on the side of a Søderberg anode. Dotted lines: equipotential lines; full lines: current paths. The bath level was positioned at −1.4 cm on the vertical scale.

used with advantage to measure the potential distribution in the bath with accurate positioning.

### 2.3. *Potential distribution*

The potential distribution in the bath was measured by connecting the electrode probe to the position sensor. The potential in an exact position could be read and stored by the attached computer. Before measuring the potentials, the ledge and anode profiles of the experimental cell were determined. The metal and bath levels were also determined at this time. In this case the probe was replaced by a steel rod which was moved along the surfaces. Figure 3 shows a typical outline of a vertical cross section of a part of a cell including the measured side ledge and anode profiles.

The potential measurements were taken in the bath between the anode and the side ledge. Positioning the probe under the curved part of the anode was difficult, so the shape of the equipotential curves in this range are rather uncertain. Between one hundred and two hundred sets of data points were measured in each experiment. Figure 4 gives an example of how these data were treated to obtain the current distribution up along the side of the anode in the bath, showing typical equipotential and current lines for the Søderberg cells under study. Smooth equipotential curves were drawn through the somewhat scattered experimental points. Drawn orthogonal to the equipotential curves, current lines along the side of the anode were presented. The current density of each current line could be calculated by the equation

$$i = \kappa \frac{\Delta V}{d} \tag{2}$$

where $i$ is the current density, $\kappa$ is the conductivity of the electrolyte, $\Delta V$ is the potential difference and $d$ is the distance between two adjacent equipotential lines.

For every current line shown in Fig. 4 we used the mean value of the two grids closest to the anode (1.6–1.2 V and 1.2–0.8 V) to represent the anode current density. In this calculation the influence of gas bubbles on the conductivity was neglected, since the gas bubbles tend to move close to the surface of the anode.

The calculated current densities represent the values at the isopotential line of 1.2 V. There is a difference in area between the anode surface and the surface along the isopotential lines. The current densities of the anode surface must be higher than those at the isopotential lines since the curved surface for current flow at this line is larger than that at the anode surface. According to the lengths of the isopotential lines and the anode curvatures, a factor (1.15) was used to multiply these current densities to give the correct current densities at the anode surface.

## 3. Results and discussion

### 3.1. *Current distribution and anode consumption*

*3.1.1. Current distribution.* Results of current distribution experiments in industrial cells are shown in Fig. 5. The curves show the current density on the side of the anode when moving downward in the vertical direction from the surface of the bath. Results for three Søderberg cells are presented with duplicate measurements for cell (B). The curves were extended to the interpolar space between the carbon anode and the aluminium cathode, where we assumed the current density to be constant and equal to the anodic current density at the horizontal working surface of the anode.

It is seen that the current density along the anode at first increased slowly with increasing distance from the surface of the bath and then showed a rapid increase near the working surface of the anode in the range where the anode surface is curved (Fig. 4).

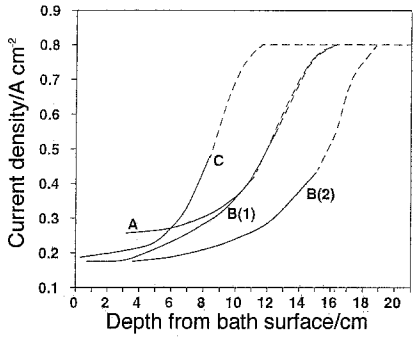


Fig. 5. Current densities on the side wall of industrial Søderberg anodes when moving downward from the surface of the bath. Anode immersion depth: cell A 16.3 cm; cell B (1) 16.2 cm; cell B (2) 18.8 cm; cell C 11.5 cm. Dotted lines are the extension of experimental data to the normal current density, 0.8 A cm$^{-2}$.

The low current density range of the Søderberg anode was located in the upper 10 cm below the bath surface, with the lowest values near the bath surface, being in the range of 0.15–0.28 A cm$^{-2}$ depending on the depth of immersion and geometry.

*3.1.2. Estimate of the amount of dust generated from the side of the Søderberg anode.* Based on the experimental results, we can estimate the amount of dust generated from the side of the Søderberg anode. The following assumptions were made: (i) dusting is uniform around the anode, depending only on current density; (ii) any dust generated through oxidation by air is disregarded; (iii) the dusting (CD) is a function of the local current density ($i$), CD $= f(i)$; and (iv) the local current density is a function of the bath depth ($z$) measured from the top of the bath, $i = f(z)$.

Laboratory results of CD [1] were expressed in percent of the theoretical carbon consumption ($W_{th}$, in g s$^{-1}$) determined by Faraday's law according to the primary cell reaction (Equation 1),

$$W_{th} = \frac{12I}{4F} \tag{3}$$

If we denote the percentage CD of $W_{th}$, the amount of carbon dust ($D$, in g cm$^{-2}$ s$^{-1}$) from the side per unit time is given by the equation (in differential form):

$$\mathrm{d}(D) = \frac{\mathrm{CD}}{100} \times W_{th} = \frac{f(i)}{100} \times \frac{12}{4F} f(z)\mathrm{d}s \tag{4}$$

where $s$ is the immersed surface area of the anode and $z$ is the vertical distance on the anode. Integrating over the surface of the anode side, the amount of carbon dust ($D_{side}$) generated from the side is given by the following equation:

$$D_{side} = \frac{12}{4F}\int_S \int f(i)f(z)\mathrm{d}s = \frac{12L}{4F}\int_0^z f(i)f(z)\mathrm{d}z \tag{5}$$

where $L$ is the circumference of the anode in the horizontal plane.

Carbon dust formed on the working face (underside) is given by

$$D_{work} = \frac{\mathrm{CD}_{norm}}{100} \times W_{th} = \frac{\mathrm{CD}_{norm}}{100} \times \frac{12}{4F}(I_{tot} - I_{side}) \tag{6}$$

where $\mathrm{CD}_{norm}$ is the CD at normal current density, and $I_{tot}$ and $I_{side}$ are the total current passing through the cell and the current passing through the side of the anode, respectively,

$$I_{side} = L\int_0^z f(z)\mathrm{d}z \tag{7}$$

The ratio of carbon dust formed on the side and on the working surface of the Søderberg anode can now be calculated, so long as the boundary between the side and the working face of the anode is defined (Fig. 4). For this study, it was defined by drawing a vertical line along the side and a horizontal line from the underside of the anode. A 45° line from the right angle at the intercept meets the anode contour at a point which was arbitrarily defined as the boundary.

Taking cell B as an example, the anode circumference was about 1720 cm and the current of the cell was 114 kA. The integrals (Equations 5 and 7) were solved numerically according to the curve for cell B (1) in Fig. 5 and the curve for dusting as function of current density [1], to obtain the amount of carbon dust coming both from the side and from the working surface:

$$D_{side} = 0.051\,\mathrm{g\,s^{-1}}; \quad D_{work} = 0.73\,\mathrm{g\,s^{-1}}$$

As a percentage of the total, the dusting from the side is

$$\frac{D_{side}}{D_{side} + D_{work}} \approx 7\% \tag{8}$$

In this case the side/bottom boundary of the anode was located 12.8 cm below the bath level, while the immersion depth of the anode was at 16.2 cm. The results achieved for the other cells were in the range of 4%–8% depending on the anode immersion depth. The major part of the carbon dust was generated from the working face, and not from the sides of the anode. This conclusion differs from the case for prebaked anodes, as claimed by Cutshall [8]. By means of Equation 7, it is found that only a small portion of the total current, 3%–6%, passes through the sides of the Søderberg anode (compared to the working face of the anode) as defined here. It is therefore logical that the major part of the dusting should occur at the working surface (bottom).

### 3.2. *Carbon consumption on the sides of Søderberg anodes*

On the sides of a Søderberg anode, carbon consumption takes place in two different ways: that is, air burning above the bath level and electrolytic consumption below the bath level. Although the latter was discussed above, both were investigated by another

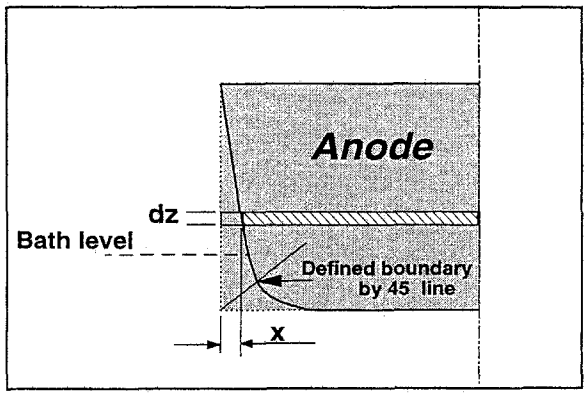


Fig. 6. Model on anode side carbon consumption.

approach. With the position sensor, the total anode side contour could be measured, hence the carbon consumption could be estimated.

Figure 6 shows a model of this estimation. In the graph, the shaded area is the original size of the anode. Due to the air burning above the bath and the electrolytic consumption in the bath, the side of the anode is reduced by gradual consumption as it moves downwards to the working face, so it has the shape of the curvature inside the shaded area. If the thickness of the consumed part, $x$, is known at a certain position, the mass consumed in that vertical position can be expressed as follows:

$$m = \Delta V \rho = [WL\mathrm{d}z - (W - 2x)(L - 2x)\mathrm{d}z]\rho \quad (9)$$

where dz here refers to a differential in the vertical direction of the anode; $W$ and $L$ are the width and length of the anode respectively; $\Delta V$ is the volume of the consumed anode material; $\rho$ is the bulk density of the anode while $m$ is the mass of the consumed part of the anode.

If the consumed mass is referred to the ratio of the total mass, $M$,

$$\frac{m}{M} = \frac{\Delta V \rho}{V \rho} = 1 - \frac{(W - 2x)(L - 2x)}{WL} \quad (10)$$

where $V$ and $M$ are the total volume and mass of the anode in a differential height (dz), respectively.

The position sensor was used to determine the wear ($x$) at the side of the anode. Figure 7 represents a typical shape of a measured Søderberg anode. The curvature of the anode was measured downward from the lower end of the anode casing. The point near the casing was taken as the reference position of the unconsumed anode.

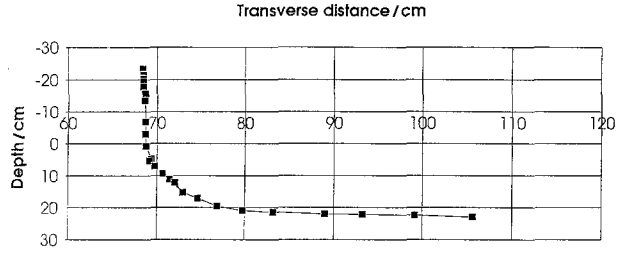


Fig. 7. Typical shape of a Soderberg anode, bath level at 9.6 cm, side/bottom boundary at 12.6 cm.

*Table 1. Measured data of carbon consumption on the side of industrial Søderberg anodes*

| No. | $x_1^*$/mm | $x_2^*$/mm | $C_{burn}^{\dagger}$/% | $C_{tot,s}^{\dagger}$/% | $C_{el}^{\dagger}$/% |
|---|---|---|---|---|---|
| 1 | 29 | 38 | 3.6 | 4.7 | 1.1 |
| 2 | 24 | 40 | 3.0 | 4.9 | 1.9 |
| 3 | 26 | 35 | 3.2 | 4.3 | 1.1 |
| Average | | | 3.3 | 4.6 | 1.3 |

* $x_1, x_2$: measured data, at bath level and at the side/bottom boundary, respectively

† $C_{burn}$, $C_{tot,s}$: consumption of anode on the side, carbon burn-off and total consumed in the side, while $C_{el}$ is the electrolytic consumption in the side ($C_{el} = C_{tot,s} - C_{burn}$).

From the curvature of the anode the consumed part of carbon on the side, $x$, could be determined. The bath level of the cell divided the air burning zone and the electrolytic consumption zone. Using the definition of the boundary between the side and the bottom of the anode (see the previous section), we obtained the wear of carbon on the side of the anode, $x$, below the bath level by electrolytic consumption. A series of experimental data and the results are listed in Table 1.

It should be understood that the air burn-off and the electrolytic consumption in the Table also include consumption due to the Boudouard reaction by passage of the anode gas. The anode gas is collected and led to the exhaust gas control system using a slight underpressure. Some air will be sucked under the gas collecting channel, and this air may cause some air burn. The total consumed carbon on the side, $C_{tot,s}$, thus may have four sources: that is, the air burn, the Boudouard reaction, the electrolytic consumption and dusting.

From the Table we see that about 3.3% of the anode carbon was burned off, which is somewhat less than data (4%–5%) given by Foosnæs and Naterstad [11]. This difference may depend on the design of the gas collecting system, the suction applied, the quality of the anodes etc.

The results show that only about 5% of the total carbon mass was consumed in the side part of the Søderberg anode. This supports our estimate in the previous section that the major part of the carbon dust was generated from the working surface, and not from the side of the anode (previous section).

## 5. Conclusions

The current density decreases in the upward direction along the side wall of an industrial Søderberg anode. The lowest current density is located at the upper part of the anode below the bath, and it ranges from 0.15 to 0.28 A cm$^{-2}$.

Only about 5%–10% of the carbon dust generated in Søderberg cells comes from the side of the anode, the rest comes from the working surface.

Air burning represents about 3% of the total carbon consumption for Søderberg anodes, while in total, 5% of the carbon was consumed in the side of the anode.

**Acknowledgements**

Financial assistance from The Royal Norwegian Council for Scientific and Industrial Research (NTNF) in cooperation with the Norwegian aluminium industry is gratefully acknowledged. Thanks are due to Dr K. Tørklep and T. Nordbø of Elkem Research a.s for help to use the position sensor and to the management of Elkem Aluminium, Moskøen for permission to carry out measurements on industrial Søderberg cells (115 kA). The help of H. Gudbrandsen of SINTEF for making the reference electrode is gratefully appreciated.

**References**

[1] Z. Kuang, J. Thonstad and M. Sørlie, *Light Metals* (1994) 667.
[2] Z. Kuang, 'On the Consumption of Carbon Anodes in Aluminium Electrolysis', PhD thesis (1994), The Norwegian Institute of Technology.
[3] J. Thonstad, *J. Electrochem. Soc.* **111** (1964) 959.
[4] L. N. Solli, 'Carbon Anodes in Aluminium Electrolysis Cells. Factors Affecting Anode Potential and Carbon Consumption', PhD thesis (1994), The Norwegian Institute of Technology.
[5] W. E. Haupin, *J. Metals* **23** (1971) 46.
[6] J. Thonstad and S. Rolseth, Proceedings of Molten Salts Symposium (1976), The Electrochemical Society, p. 393.
[7] S. Rolseth, A. Solheim and J. Thonstad, Proceedings of International Symposium on Reduction and Casting of Aluminium (edited by C. Bickert), Montreal, Canada, Pergamon (1988) p. 229.
[8] E. R. Cutshall, *Light Metals* (1986) 629.
[9] K. Tørklep, *Light Metals* (1994) 1205.
[10] J. Thonstad and S. Rolseth, *Electrochim. Acta* **23** (1978) 223.
[11] T. Foosnæs and T. Naterstad, 'Carbon: Basics and Principles' *in* 'Introduction to Aluminium Electrolysis' (edited by K. Grjotheim and H. Kvande, Aluminium-Verlag, Düsseldorf (1993).